Saudi Journal of Biological Sciences 29 (2022) 1832–1841

Contents lists available at ScienceDirect

Saudi Journal of Biological Sciences

journal homepage: www.sciencedirect.com

Original article

Novel Clotrimazole and *Vitis vinifera* loaded chitosan nanoparticles: Antifungal and wound healing efficiencies

Esraa E. Elshaer [a], Bassma H. Elwakil [b,*], Areej Eskandrani [c], Salma S. Elshewemi [d], Zakia A. Olama [a]

[a] Botany and Microbiology Department, Faculty of Science, Alexandria University, Alexandria 21500, Egypt
[b] Medical Laboratory Technology Department, Faculty of Applied Health Sciences Technology, Pharos University in Alexandria, Alexandria 21500, Egypt
[c] Chemistry Department, College of Science, Taibah University, Madinah 30002, Kingdom of Saudi Arabia
[d] Zoology Department, Faculty of Science, Alexandria University, Alexandria 21500, Egypt

ARTICLE INFO

Article history:
Received 13 August 2021
Revised 8 October 2021
Accepted 15 October 2021
Available online 22 October 2021

Keywords:
Clotrimazole
Egyptian *Vitis vinifera*
Chitosan Nanoparticles
Wound Healing

ABSTRACT

Chitosan integrated nanoparticles of clotrimazole and Egyptian *Vitis vinifera* juice extract was evaluated in order to maximize the antifungal activity and reduce the gross side effects. In the present study Egyptian Thompson Seedless *Vitis vinifera* and Clotrimazole (Cz) loaded chitosan nanoparticles (NCs/VJ/Cz) showed a promising antifungal effect with average inhibition zone diameters of 74 and 72 mm against *Candida albicans* and *Aspergillus niger* respectively. NCs/VJ /Cz was stable with significant drug entrapment efficiency reached 94.7%; PDI 0.24; zeta potential value + 31 and average size 35.4 nm diameter. Ex vivo and in vivo evaluation of skin retention, permeation and wound repair potentialities of NCs/VJ /Cz ointment was examined by experimental rats with wounded skin fungal infection. Data proved the ability of NCs/VJ /Cz to gradually release the drugs in a sustained manner with complete wound healing effect and tissue repair after 7 days administration. As a conclusion NCs/VJ /Cz ointment can be used as a novel anti-dermatophytic agent with high wound healing capacity.

1. Introduction

Dermatophytosis are keratinophylic fungi that affect skin, hair, and nails superficially. *Cryptococcus neoformans, Candida* and *Aspergillus* species have been found to be the most common fungi causing systemic mycosis which was considered as a cause of high morbidity and mortality rates (Fuentefria et al., 2018). In order to overcome dematophytic infection, imidazoles (e.g., bifonazole, clotrimazole, miconaole) were the most commonly used antifungal drugs for the treatment of superficial cutaneous mycoses infections. Precautionary measures must be taken in the application of all fungal drugs with fungistatic mechanism of action due to high toxicity, insufficient bioavailability and the development of resistance by fungal pathogens or emerging innate resistance among fungal species' (Cavaleiro et al., 2015). Search for a novel antifungal drug will be necessary for the future, natural products are important source for new therapeutic agents of different strategies that can be applied to improve the antifungal drugs.

Grapes (*Vitis vinifera*) are cultivated especially on the Mediterranean area (Falah-Tafti, 2010). *Vitis vinifera* juice extract facilitates and accelerate skin wound healing with antioxidant, antimicrobial, antiviral and anti-cancer activities (Nassiri-Asl & Hosseinzadeh, 2009). On the other hand, Chitosan is a polysaccharide (deacetylated from chitin) which has unique properties offering many industrial and biomedical applications. Chitosan nanoparticles may increase the solubility and enhance the bioavailability of different active agents, with the ability of modulating a drug targeted nano-system (Leonida et al., 2018). Chitosan nanoparticles are among biodegradable polymers which were studied extensively as delivery systems with controlled release of active ingredients (Divya & Jisha, 2018). Chitosan nanoparticles have the ability to cross different biological barriers and deliver the drug in a controlled release manner to the target site, improve the drugs bioavailability, drugs pharmacokinetics modification and to protect the loaded drugs (Divya & Jisha, 2018). The small nanoparticles size also enhance the interfacial interaction with the target cell membrane caused by the endocytosis effect (Ghadi et al., 2014; Reina et al., 2019). These properties favored the chitosan nanoparticles with several clinical potentialities to concur the

* Corresponding author.
E-mail address: bassma.hassan@pua.edu.eg (B.H. Elwakil).

Peer review under responsibility of King Saud University.

Production and hosting by Elsevier

https://doi.org/10.1016/j.sjbs.2021.10.041
1319-562X/

increasing incidence of microbial resistance (Landriscina et al., 2015).

The present study aimed to synthesize a novel drug derived from the combination between clotrimazole and Thompson seedless *Vitis vinifera* juice extract loaded chitosan nanoparticles against infectious skin mycosis.

2. Material and methods

2.1. Vitis vinifera (Grape) samples

Vitis vinifera samples namely: Thompson (VJ) and Flame seedless (FJ) *Vitis vinifera* were collected during September 2019, from Alexandria, Egypt. The samples were cleaned and rinsed with sterile water then air dried.

2.2. Microorganisms

Some dermatophytes namely: *Aspergillus niger, Aspergillus Flavus, Fusarium oxysporum, Candida albicans*, *Mucor hiemalis* and a standard strain *Candida albicans* ATCC 14,053 were kindly identified and provided by Assiut University Mycological Center (AUMC) (Mousafa, 2006).

2.3. Seed culture preparations

Spore suspension and yeast seed culture were prepared according to CLSI guidelines (CLSI, 2017).

2.4. Preparation of the Vitis vinifera juice extract

Vitis vinifera samples were macerated and extracted using an alcoholic solvent (water/ethanol: 20/80 v/v) at 60 °C for 1 hr then filtered through a Whatman filter paper No. 1 (Katalinic et al., 2013).

2.5. Antifungal activity of Vitis vinifera juice extract

Antifungal activity of all the prepared extracts was evaluated by disc-diffusion method using Potato dextrose agar (PDA) plates (Oliveira et al., 2013).

2.6. Combination between grape juice extracts and the commonly used antifungals

Clotrimazole (Cz), and Fluconazole (Flz) discs were loaded with 25 μl of *Vitis vinifera* juice extracts one at a time and was applied on the surface of the PDA fungal inoculated plates (Nirmala & Narendhirakannan, 2011). Further evaluation of the combination efficacy was done using minimum inhibitory concentration (MIC), minimum fungicidal concentration (MFC) and checkerboard dilution technique (Foucquier & Guedj, 2015).

2.7. Chemical analysis of Thompson Seedless Vitis vinifera juice extract (VJ)

2.7.1. GC–MS analysis

Thompson Seedless *Vitis vinifera* juice extract (VJ) was subjected to GC–MS analysis using capillary column SBP5 (30 m × 0.32 mm × 0.25 μm) installed in a Hewlett-Packard 5890 Series II instrument (Nirmala & Narendhirakannan, 2011). GC–MS analysis was done at National Institute of Oceanography and Fisheries, Alexandria University, Egypt.

2.8. Nanoparticles preparation

2.8.1. Nano-chitosan preparation (NCs)

Nano-chitosan (NCs) was prepared using ionic gelation method according to Elnaggar et al. (2020) using sodium TPP solution (0.2% w/v in deionized water).

2.8.2. Nano-chitosan /Thompson Seedless Vitis vinifera juice extract (NCs/VJ)

NCs encapsulated with VJ (20 mg) were prepared using incorporation method according to Ong et al. (2017).

2.8.3. Nano-chitosan/Clotrimazole (NCs/Cz)

NCs encapsulated with Cz (10 mg) was prepared using incorporation method according to Koukaras et al. (2012).

2.8.4. Nanochitosan /Thompson Seedless Vitis vinifera /Clotrimazole (NCs/VJ/Cz)

NCs encapsulated with Cz (10 mg) and VJ (20 mg) were prepared by mixing Cz and VJ with the prepared TPP solution under stirring. The mixture was added drop-wise into two different chitosan concentrations (0.25 and 0.5%) one at a time to reach higher loading efficiency. The prepared nanoparticles were stored at 4C in sterile falcon tubes after centrifugation and lyophilization for further investigations.

2.9. Antifungal activity of the prepared nanoformulae

The prepared Nano-formulae (NCs, NCs/VJ, NCs/Cz and NCs/VJ/Cz) were evaluated using disc-diffusion method; MIC, and MFC (Nina et al., 2015). *Candida albicans* treated cells with the most promising formula were examined using transmission electron microscopy (TEM) using a Transmission Electron Microscope (JEM-100 CX Joel) at the Electron Microscope Unit, Faculty of Science, Alexandria University, Egypt. While *A. niger* treated hyphae was examined using light microscope (Ribes et al., 2017).

2.10. Test for antioxidant (DPPH scavenging) activity

The DPPH (2,2- diphenyl-1-picryl-hydrazyl) scavenging effect was calculated using the following equation:

$$Scavengingpercentage = \frac{ADPPH - AS}{ADPPH} \times 100$$

where AS is the absorbance of the solution when the sample under test has been added at a particular concentration and ADPPH is the absorbance of the DPPH solution (Xie et al., 2015).

2.11. Characterization of the most promising nanoformula

The ultrastructure, size and shape of the prepared nanoformulae were examined using TEM (JEM-100 CX Joel) (Vinodhini et al., 2017). FTIR (FTIR-BRUKER, wave number ranged from 4000 cm^{-1} to 450 cm^{-1}) was used to investigate the nanoparticles functional groups and X-Ray diffraction (XRD-BRUKER AXS, Cu Kα radiation source (λ = 0.154 nm), at scan rate = 10/ min) of the most promising nanoformula were analyzed (Elnaggar et al., 2020). However, the particle size (PS), polydispersity index (PDI) and Zeta potential of the most promising Nano-formula was determined by dynamic light scattering (DLS) technique (Malvern Zetasizer) (Elnaggar et al., 2020).

The entrapment efficiency of the most promising nanoformula was investigated according to El-Refaie et al. (2015). The entrapment efficiency percentage (EE%) was calculated using the following equation:

$$EE\% = \frac{Totalunentrappeddrug}{Totaldrug} \times 100$$

Finally, the release of Clotrimazole and Thompson seedless *Vitis vinifera* juice extract were determined using dialysis bag (2.5 cm in diameter) at different time intervals (0.5, 1, 2, 3, 4, 5 and 6 hrs) according to El-Refaie et al. (2015). Cz and VJ release% were calculated and drug concentration was measured with UV absorbance at 237 and 280 nm respectively (Bonazzi et al., 1998; Xiao et al., 2018)

2.12. Ointment preparation

Four grams of gelatin powder was dissolved in 100 ml distilled water at 40 °C for 30 min. After complete homogenization, the gelatin solution was incorporated with 500 mg/ml of each VJ loaded chitosan nanoparticles, Cz loaded chitosan nanoparticles and the most potent formula (NCs/VJ/Cz) one at a time and mixed with constant stirring for 1 h at 4 °C (Jridi et al., 2017).

2.13. Formula evaluation using animal model

2.13.1. Ex vivo permeation studies

2.13.1.1. Preparation of skin samples. Ethics Committee at the Faculty of Science, Alexandria University, Egypt has approved the present experiment (ALEXU IACUC Institutional Animal Care and Use Committee on research (AU04190413302). The animals were kept under standard laboratory conditions and veterinary supervision with access to water and food ad libitum. Thiopental solution (40 mg/kg) was injected intraperitonealy for rat anesthetization (IACUC Faculty and Staff, 2016). Shaving razor was used for the removal of the rats' dorsal hair carefully (Butani et al., 2014). The hypodermis part of the shaved skin was removed with scalpel (Aggarwal, 2006) which was then washed with saline and stored in refrigerator (−20 °C) until use (Sahoo et al., 2014).

2.13.1.2. Skin permeation studies. Franz diffusion cells (surface of 3.14 cm^2 and volume = 9 ml) were used in the ex vivo release studies of Egyptian Thompson seedless *Vitis vinifera* (VJ) and Clotrimazole (Cz) from the prepared ointment (NCs/VJ/Cz ointment). 9 ml of sodium phosphate buffer (SPB) of pH 5.5 was poured into the Franz diffusion cells' receptor compartment at 32 °C ± 0.5 °C (Kumar et al., 2014). The excised skin was placed between the receptor compartment and the donor of the Franz diffusion cell (Song et al., 2014). The ointment (0.5 g) was applied uniformly on the excised skin. Then at different time intervals (2, 4, 6, 8, 10, 12, and 24 h) a 2 ml aliquot was withdrawn (replaced with freshly prepared SPB medium) and filtered. Each aliquot was analyzed using UV–vis spectrophotometer at 237 and 280 nm respectively (Bonazzi et al., 1998; Xiao et al., 2018) to calculate the percentage of cumulative Cz and VJ drug permeated through the rats' excised skin.

2.13.1.3. Skin retention study. After ending the permeation studies the excised skin was separated and washed with methanol then the excised skin was vortexed in SPB. For effective extraction of the retained VJ and Cz, each skin sample was immersed in methanol for 24 hrs under shaking condition (100 rpm at 37 °C) (Song et al., 2012; Butani et al., 2014). Each sample was then sonicated and centrifuged (8000 rpm) for 20 min (Verma et al., 2014). The supernatant was analyzed with a UV method at 237 and 280 nm respectively (Bonazzi et al., 1998; Xiao et al., 2018) and the placebo nanoparticles was used as a blank (Ge et al., 2014). The percentage of Cz and VJ deposition were calculated and represented as average ± SD.

2.13.2. In vivo studies.

2.13.2.1. In vivo skin retention study. In vivo skin retention study was carried out according to Aggarwal & Goindi (2013). Male rats (*Rattus norvegicus albinus*) weighing 195 ± 30 g were anesthetized using intraperitoneal injection using 10 mg/kg xylazine and 80–100 mg/kg hydrochloride (Gupta & Vyas, 2012; Altuntas et al., 2014). Shaving razor was used to shave the rats' dorsal hair carefully (Butani et al., 2014). Half (0.5) g of the prepared ointment of NCs/VJ/Cz was applied on the shaved area. The animals were sacrificed after 5 min, then after 2, 4, 6, and 24 hrs. The shaved dorsal skin was excised and washed with methanol. Skin preparation was done as described in the ex vivo drug retention study to assess the deposition of VJ and Cz using UV–vis spectrophotometer at 237 and 280 nm respectively (Bonazzi et al., 1998; Xiao et al., 2018).

2.13.2.2. In vivo antifungal activity of NCs/VJ/Cz ointment. In vivo antifungal activity study of NCs/VJ/Cz ointment was done following Gupta and Vyas (2012).

2.13.2.2.1. Animal preparation. Fifty-five male albino rats (*Rattus norvegicus albinus*), 4 months old with average body weight of 180 ± 30 g were assigned to eleven groups each including 5 rats and kept in a cage under conventional conditions of temperature and humidity in separate cages in average temperature (25 ± 2C) inside an adequately ventilated room (Elsheikh et al., 2012).

Dorsal inter-scapular region of each albino rat was disinfected with ethanol (70%) and shaved one day prior to infection. All experiment was done under aseptic conditions. A circular wound was created by excising the skin carefully with a 15-mm biopsy punch; circular wounded areas were left open until the end of the experiment (Tramontina, 2002). Aliquots of $1x10^6$-10^8 *A. niger* spore suspension was injected intradermally in the wounded area (Qushawy et al., 2018).

However, treatment regimen began 72 hrs post-fungal infection where test formulations were topically applied once daily (0.5 g/day) for three consecutive days. The rats were divided into eleven groups according to their treatment regimen as follows:

Group I: Assigned as negative control with neither fungal infection nor treatment regimen.

Group II: Assigned as positive control, infected with *A. niger* strain with no treatment regimen.

Group III: *A. niger* Infected rats treated with gelatin solution only.

Group IV: *A. niger* Infected rats treated with NCs placebo only.

Group V: *A. niger* Infected rats treated with Cz only.

Group VI: *A. niger* Infected rats treated with VJ only.

Group VII: *A. niger* Infected rats treated with the combination of Cz and VJ.

Group VIII: *A. niger* Infected rats treated with ointment I (**NCs/VJ**: gelatin (1:1 w/v)).

Group IX: *A. niger* Infected rats treated with ointment II (**NCs/Cz**: gelatin (1:1 w/v)).

Group X: *A. niger* Infected rats treated with ointment III (**NCs/VJ/Cz**: gelatin (1:1 w/v)).

Group XI: Assigned as the treatment control (ointment III) with no infection (toxicity assessment).

The progressive changes in wound area were monitored, and measured every day. The percentage of contraction was calculated by the following formula:

$$Percentageofcontraction = 100 - \left(\frac{Woundareaonthelastday}{Woundareaonthefirstday} \times 100\right)$$

Rats were checked twice daily during the experimental period to ensure no adverse reactions were observed. This is the first work to emphasis the effect of NCs/VJ/Cz conjugated nanoparticles as a treatment for wounded skin fungal infection in rats.

2.13.2.2.2. Histological studies. The excised healed skin tissue of each rat group was fixed in 10% formalin to allow good fixative penetration for histological examination. Sections (5 μm thick) were stained with Ehrlich's hematoxylin and counterstained with eosin (H&E). The selected sections were examined with light microscope and photographed (Arizmendi et al., 2014).

2.14. Hemocompatibilty test

Estimation of hemocompatibilty of the most promising formula was performed through Hemolysis studies using fresh human blood, collected in EDTA tube and then diluted with normal saline solution (2 ml blood + 2.5 ml normal saline) according to Basak et al. (2018). The hemolysis percentage was calculated according to following equation:

$$\%\text{Hemolysis} = \frac{\text{ODtest} - \text{ODnegative}}{\text{ODpositive} - \text{ODnegative}} \times 100$$

According to Basak et al. (2018), if the hemolysis % was less than 5% then the tested drug was considered highly hemocompatible. If the hemolysis % was within 10 , the tested drug was considered hemocompatible. On the other hand, if the hemolysis %was more than 20, the drug was reported as non hemocompatible.

2.15. Statistical analyses

All experiments were performed in triplicates and results were expressed as Mean ± Standard Deviation. Statistical analysis was performed by SPSS 16.0.

3. Results

3.1. Antifungal activity of Egyptian grape juice extract

Data in Table 1 showed that Flame Seedless *Vitis vinifera* juice extract (FJ) reported higher antifungal activity than Clotrimazole (Cz) and Thompson Seedless *Vitis vinifera* juice extract (VJ). It was revealed that *A. niger* and *Candida albicans* were the most resistant strains against the tested agents with inhibition zone diameter of 12.12 and 10.37 mm respectively.

3.2. Combination between Vitis vinifera juice extract and some antifungal agents

Data in Table 2 revealed that the antifungal effect of Cz/VJ showed significantly higher antifungal activity (Inhibition Zone diameter: 61.16 mm) than other combinations against the tested dermatophytes. Data revealed that Flame Seedless *Vitis vinifera* juice extract showed antagonistic effect with the tested antifungal agents while Thompson Seedless *Vitis vinifera* juice extract (VJ) showed a promising synergistic effect. VJ was selected for further studies. The combined antifungal activity of VJ and Cz were further evaluated by the checkerboard dilution technique. It was revealed that VJ/Cz had a synergistic effect with FICI equaled 0.5 against both *A. niger* and *Candida albicans*.

3.3. GC/MS analysis of Thompson Seedless Vitis vinifera juice extract

Thompson seedless *Vitis vinifera* juice extract was prepared and analyzed using GC–MS (Fig. 1). hydroxymethyl furfural, 5,3-Hydroxy-2,3-dihydromaltol, and ethyl-2-hydroxymethylimidazole (7, 13 and 80% respectively) had been identified on referring to the corresponding acquisition time. Other compounds were detected in lower concentrations (e.g. eugenol 4% and α-terpineol 0.01).

3.4. The antifungal effect of the synthesized nanoparticles

Data in Table 3 revealed that NCs (0.25%)/VJ/Cz was the most promising formula with inhibition zone diameter of 72 and 74 mm against *A. niger and Candida albicans* respectively and therefore it was used for further studies. Other tested chitosan concentrations gave inferior results.

3.5. Determination of MIC, MFC and MIC index of the most promising formula

Table 4 revealed that the MIC that led to the maximum inhibition was reported with NCs/VJ/Cz nanoformula (2 μg/ml). According to the MIC index values, it was revealed that VJ alone had a Fungistatic effect but after the formula incorporation the effect was converted to Fungicidal effect due to the interaction between VJ, Cz and NCs.

3.6. Microscopic examination of fungal treated cells

It was observed that the formula was precipitated and adsorbed on the cell surface leading to cell deformation followed by cell membrane disruption, releasing the cellular contents and became as a ghost cell (Fig. 2**a and b**). On the other hand, Light microscopic examination of *A. niger* treated cells showed deformed filamentous forming ghost shape (Fig. 2**c and d**).

3.7. Antioxidant activity of the prepared formula

Data in Table 5 revealed that the DPPH activity% of **NCs/VJ/Cz** was 97.5% with IC_{50} 2.7 mg/ml.

3.8. Characterization of the synthesized nanoparticles

3.8.1. Transmission electron microscopic examinations

TEM images (Fig. 3) illustrated that the prepared NCs had a vesicle size ranged between 216 and 263 nm, upon the addition of VJ the vesicle size was 59–124 nm. On the other hand, NCs/Cz showed relatively low vesicle size (67–75 nm) while NCs/VJ/Cz had a vesicle size between 50 and 89 nm. The prepared nanoparticles had a denser color in the core.

Table 1
Antifungal activity of Egyptian Seedless *Vitis vinifera* juice extract and some some pharmaceutical products.

Organism / Antifungal agent	Average inhibition zone diameter (mm) ± Standard deviation			
	Thompson Seedless (VJ)	Flame Seedless (FJ)	Clotrimazole (Cz)	Fluconazole (Flz)
A. niger	13.6 ± 0.25	13.6 ± 0.28	6.1 ± 0.02	15.2 ± 0.55
A. flavus	15.6 ± 0.28	14.2 ± 0.72	10.0 ± 0.10	17.8 ± 0.67
Fusarium oxysporum	17.8 ± 0.28	26.6 ± 0.28	11.0 ± 0.11	17.7 ± 0.71
Candida albicans ATCC	14.9 ± 0.46	17.2 ± 0.50	11.0 ± 0.11	16.4 ± 0.68
Candida albicans	12.6 ± 0.76	11.4 ± 0.5	6.0 ± 0.1	11.5 ± 0.67
Mucor hiemalis	17.0 ± 0	21.0 ± 0.59	11.2 ± 0.1	± 0.66

Table 2
Combination study of different Egyptian Seedless *Vitis vinifera* juice extracts with some pharmaceutical products

Organism combination trial	Average inhibition zone diameter (mm) ± Standard deviation					
	A. Niger	*A. Flavus*	*Fusarium oxysporum*	*Candida albicans ATCC*	*Candida albicans*	*Mucor hiemalis*
Fluconazole/FJ	20.0 ± 0.10	30.0 ± 0.20	30.0 ± 0.10	30.0 ± 0.10	21.0 ± 0.10	25.0 ± 0.15
Clotrimazole/FJ	15.0 ± 0.10	23.0 ± 0.15	22.0 ± 0.20	20.0 ± 0.10	16.0 ± 0.20	20.0 ± 0.20
Fluconazole/ VJ	29.0 ± 0.15	35.0 ± 0.10	37.0 ± 0.10	31.0 ± 0.10	25.0 ± 0.15	40.0 ± 0.15
Clotrimazole / VJ	60.0 ± 0.20	74.0 ± 0.30	60.0 ± 0.20	77.0 ± 0.20	66.0 ± 0.15	30.0 ± 0.20

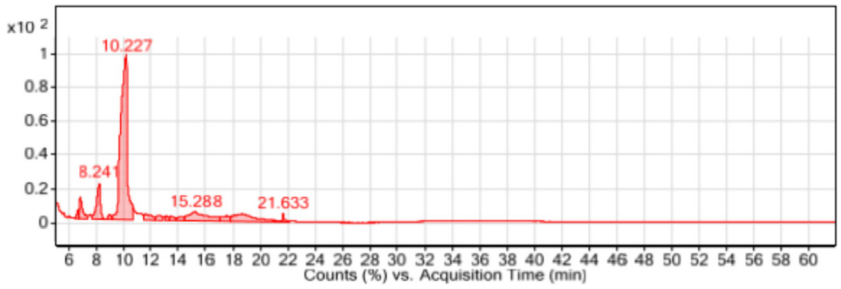

Fig. 1. GC/MS analysis of Thompson Seedless *Vitis vinifera* juice extract (VJ).

Table 3
Antifungal effect of the synthesized nanoparticles

Nano formulae	Average inhibition zone diameter (mm) ± Standard deviation	
	A. niger	*Candida albicans*
NCs (0.25%)(control)	6.0 ± 0	6.0 ± 0
NCs (0.5%)(control)	6.0 ± 0	6.0 ± 0
NCs (0.25%)/VJ	17.33 ± 1.15	14.33 ± 0.57
NCs (0.5%)/VJ	14.33 ± 0.57	15.0 ± 1
NCs (0.25%)/Cz	11.66 ± 0.57	20.0 ± 1
NCs (0.5%)/Cz	12.0 ± 1	14.0 ± 0.57
NCs (0.25%)/VJ /Cz	72.0 ± 1	74.0 ± 1.5
NCs (0.5%)/VJ/Cz	60.33 ± 1.15	66.0 ± 1

3.8.2. Fourier transform infrared spectroscopic (FTIR) analysis and X-Ray diffraction

FTIR spectral details of NCs/VJ/Cz (Fig. 4**a)** showed absorption band obtained at 3433.9 cm^{-1} attributed to a collective –NH and OH group resulted in a broadened band due to the physical interactions with TPP when converting chitosan to a Nano particulate form. The peak at 1730.15 cm^{-1} was assigned to the C = O and C–O which may be explained by the functionalization of eugenol and 5,3-Hydroxy-2,3-dihydromaltol on the prepared chitosan nanoparticles. Data in Fig. 4**b** showed the X-Ray diffraction patterns of NCs loaded with VJ and Cz showed two peaks at $2\Theta = 27^{\circ}$ indicating a shift from the pure chitosan peaks around 20° revealed the increased amorphous nature**.**

3.8.3. Determination of entrapment efficiency, particle size, PDI and Zeta potential

The physical characteristics of NCs/VJ/Cz formula (Table 6) revealed that the mean diameter, PDI value and Zeta potential were 35.4 nm, 0.248 and + 31 mV respectively indicating homogenous size distribution with good stability. The entrapment efficiency of VJ/Cz into the chitosan vesicles was found to be 94.7%.

3.8.4. Drug release study

NCs/VJ/Cz was able to gradually release the drug load by time. After 2 hrs, the cumulative release of VJ from the Nano carrier was 47.9 ± 1.9% compared to 35 ± 1.5% for Cz (Fig. 5). The initial burst release might be attributed to the diffusion of Cz and VJ that were localized at or close to the surface of the prepared nanoparticles.

3.9. Formula evaluation using animal model

3.9.1. Skin permeation study

Ex vivo permeation studies of Egyptian Thompson Seedless *Vitis vinifera* (VJ) and Clotrimazole (Cz) from the loaded Chitosan nanoparticles (NCs/VJ/Cz) ointment were tested. The ex vivo release pattern of VJ and Cz was shown in Fig. 6**.** Ex vivo permeation of Egyptian Thompson Seedless *Vitis vinifera* (VJ) and Clotrimazole (Cz) was enhanced upon its incorporation into the ointment showing almost a 1.5-fold permeation increase.

Table 4
MIC and MFC of the tested formulae

Antifungal agents	MIC (μg/ml)		MFC (μg/ml)	
	A. niger	*Candida albicans*	*A. niger*	*Candida albicans*
VJ	**128.0**	**128.0**	**1000.0**	**1000.0**
Cz	**64.0**	**64.0**	**125.0**	**125.0**
NCs	**256.0**	**128.0**	**512.0**	**256.0**
VJ/Cz	**32.0**	**16.0**	**64.0**	**32.0**
NCs/VJ	**128.0**	**128.0**	**256.0**	**256.0**
NCs/Cz	**32.0**	**32.0**	**64.0**	**64.0**
NCs/VJ/Cz	**2.0**	**2.0**	**2.0**	**2.0**

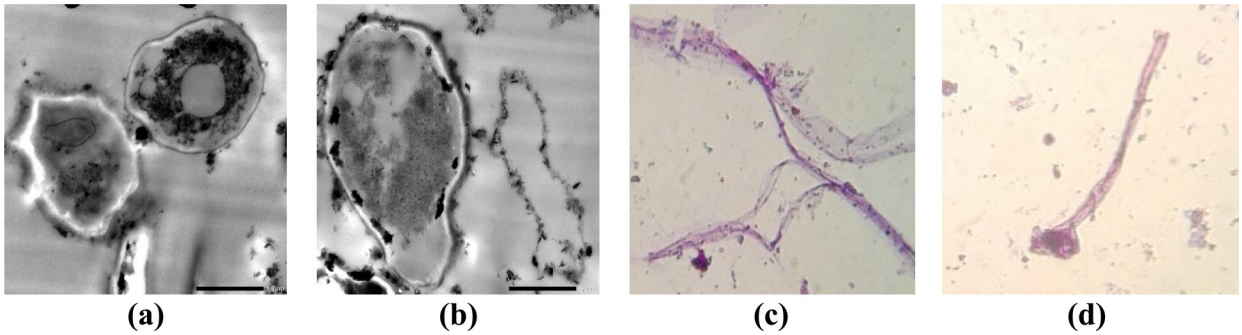

Fig. 2. Transmission Electron microscopic of *Candida albicans* treated cells (a and b) and Light microscopic examination of *A. niger* hyphal treated cells (c and d).

Table 5
Antioxidant activities of the tested formulae

Sample	IC_{50} (mg/ml)	DPPH scavenging activity (%)
VJ	90.77	25.14
NCs	120.78	15.93
Cz	150.90	7.34
NCs/Cz	104.21	19.81
NCs/VJ	32.93	74.58
NCs/VJ /Cz	2.70	97.50

3.9.2. Skin retention study

Skin retention study was performed to prove the sustained locality effect of the prepared ointment into the skin. Skin samples were harvested after ending the skin permeation study to assess the VJ and Cz deposition in the skin. VJ and Cz deposition percentage in the skin was higher than the permeated percentage. Illustration of the comparison between VJ and Cz permeated and deposited percentages was shown in Table 7.

3.9.3. In vivo studies

3.9.3.1. In vivo skin deposition study. Data represented in Table 8 revealed that the VJ and Cz exhibited rapid penetration into the skin. After 5 min application of the novel formulated ointment, 69.2 ± 0.01 and 76.9 ± 0.7 μg of VJ and Cz were deposited respectively into the skin. The novel formulated ointment afterward successfully released the drugs with sustained manner through time. It is important to mention the differences between the results of ex vivo and in vivo skin retention studies which can be explained by the blood circulation to the skin which helps in drug elimination and lowering the deposition in the skin. Hence, a hemocompatibilty study was done to confirm the formula safety upon topical application.

3.10. Histological and cytotoxicity studies

It is of considerable interest that animals from experimental groups did not exhibit any case of mortality. Wound contraction showed gradual reduction of wound area in 6 days and complete healing after 7 days (Fig. 7). Examination of light micrographs of vertical skin sections of healthy wounded rats after healing showed normal histological architecture (Fig. 8**a).** While fungal infected wounded skin, showed that the epidermal keratinocytes not completely differentiated into layers with severe inflammation (Fig. 8**b).** On the other hand, the light micrograph of fungal infected wounded skin treated with the formula **(NCs/VJ/Cz)** ointment showed more defined feature of healing. Epidermis was completely regenerated with its derivatives (Fig. 8**c).** Finally, the light micrograph of the group treated with **NCs/VJ/Cz** ointment showed normal histological architecture which proved the formula safety with no sign of inflammation, irritation or any observed side effects (Fig. 8**d).** Other groups were added to supplementary file **(From S1Fig to S8 Fig).**

3.11. Hemocompatibilty test

The limit prescribed by Brazilian law and international standards was 1% for spontaneous hemolysis**.** In this study, the hemolysis activity of the promising formula (NCs/VJ/Cz) was proved to be highly hemocompatible (0.3%).

4. Discussion

Dermatophytic infections were usually treated with imidazoles (e.g., bifonazole, clotrimazole, miconaole) however some precautionary measures must be taken due to their high toxicity, insufficient bioavailability and the development of resistant fungal pathogens (Cavaleiro et al., 2015). Novel antifungal drugs using

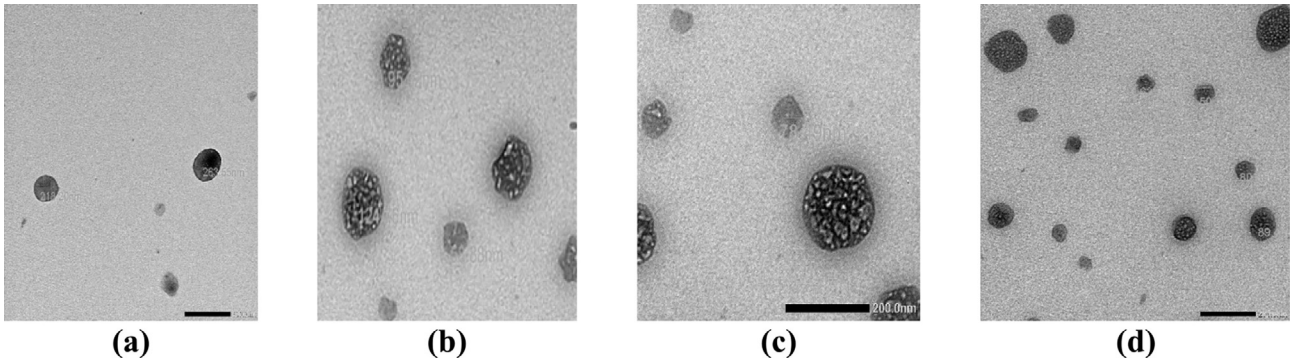

Fig. 3. Transmission Electron microscopic examination of NCs (a), NCs/VJ (b), NCs/Cz (c) and NCs/VJ/Cz (d).

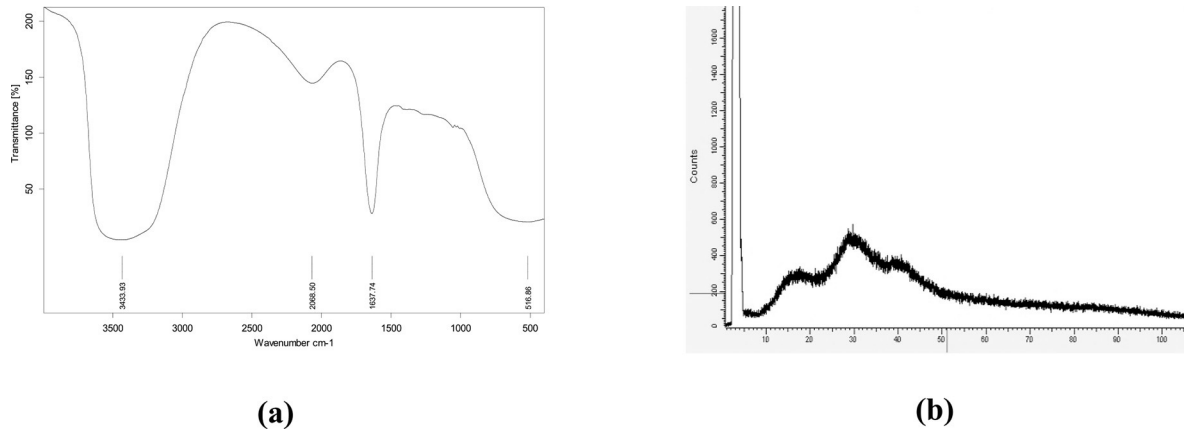

Fig. 4. FTIR analysis (a) and XRD analysis (b) of formula NCs/VJ/Cz.

Table 6
Entrapment efficiency, Particle size, PDI and Zeta potential of the selected formula

Formula	Average size (nm)	Potential	PDI	EE%
NCs/VJ/Cz	**35.40**	**+31.00**	**0.24**	**94.70**

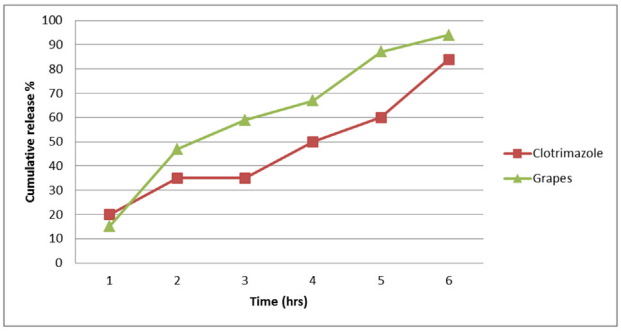

Fig. 5. In vitro drug release profile of VJ and Cz from NCs/VJ/Cz.

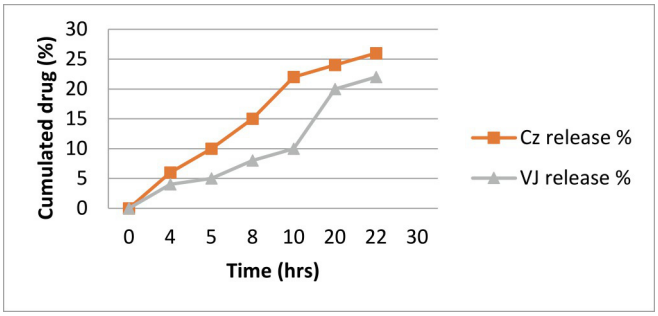

Fig. 6. Ex vivo skin permeation of VJ and Cz using the Franz diffusion cell method.
Note: The values were expressed as average ± SEM (n=3).

Table 8
In vivo skin deposition profile

Time (hrs)	Deposition (μg)	
	VJ	Cz
0.08	69.2 ± 0.01	76.9 ± 0.70
2	60.7 ± 1.00	70.1 ± 1.50
4	54.1 ± 1.10	51.9 ± 0.80
6	43.9 ± 0.50	38.3 ± 1.00
24	28.4 ± 1.50	19.7 ± 2.40

natural products has been the last resort in treating dermatophytic infections. Grapes (*Vitis vinifera*) are known to facilitate and accelerate skin wound healing with antioxidant, antimicrobial, antiviral and anti-cancer activties (Nassiri-Asl & Hosseinzadeh, 2009). In the present work, *Vitis vinifera* reported higher antifungal activity than clotrimazole (Cz). This can be explained by the high amounts of polyphenols in *Vitis vinifera* (VJ) that may play a major role in the observed antifungal effects (Fraternale et al., 2015). Houillé et al. (2014) revealed that two dimethoxy-resveratrol derivatives (3,4′-dimethoxy-resveratrol and 3,5-dimethoxyresveratrol) displayed interesting antifungal activities with minimum inhibitory concentration (MIC) values of 28–37 μg/ml against *Candida* species. Consequently, the observed antifungal activity of VJ in the present study can be reverted to the presence of dimethoxy-resveratrol derivatives. Kuruc & Čonková (2017) tested the in vitro antifungal activity of an ethanolic extract of *Vitis vinifera* tendrils (TVV) and it was revealed that the MIC values was from 250 to 300 ppm. Simonetti et al. (2019) evaluated the antifungal activity of *Vitis vinifera* extracts and it was revealed that the MIC

Table 7
In vitro and ex vivo release profile of VJ and Cz

Formula used	VJ release percentage*	Cz release percentage*	VJ permeation percentage**	Cz permeation percentage**	VJ retention percentage**	Cz retentionpercentage**
NCs/VJ/Cz	59.4 ± 0.2	34.8 ± 0.3	1.2 ± 0.4	2.4 ± 0.02	3.0 ± 0.07	5.6 ± 0.1
VJ[1]	92.2 ± 0.01		–		–	
Cz[2]	81.9 ± 0.05		–		–	

*: Dialysis bag, **: Skin, –: Not tested, [1]: VJ control and [2]: Cz control

Fig. 7. Photographs demonstrating morphological appearance of wounds after NCs/VJ/Cz treatment.

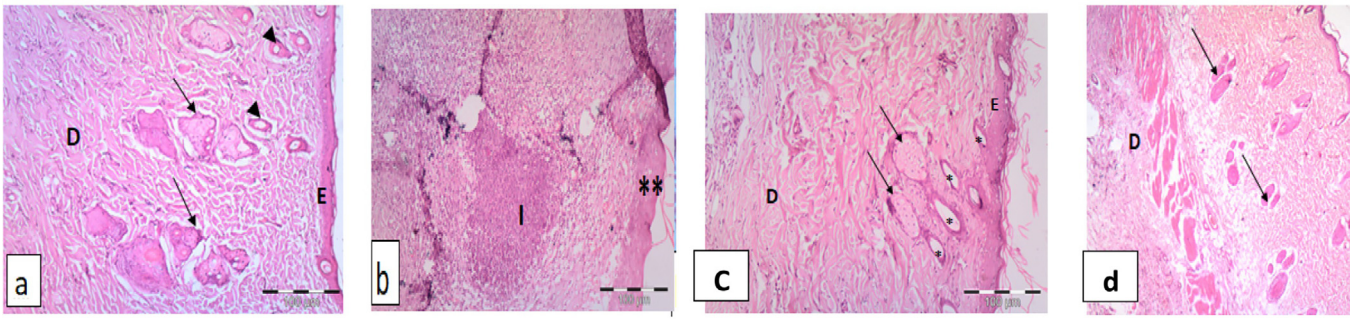

Fig. 8. Light micrographs of rats group I (a) group II (b) group X (c) and group XI (d) showing dermis (D), hair follicle (arrowheads), sebaceous gland (arrows) and epidermis (E) epidermal keratinocytes not completely differentiated into layers (**), hair follicle (*) and severe inflammatory cells (I) in newly formed dermis (X 100).

values ranged from 53.58 to 214.31 μg/ml against *Candida* spp. and from 43.54 to 133.02 μg/ml against dermatophytes. Kuruc & Čonková (2017) revealed that the efficacy of antimycotics can be increased by a proper combination between commercial drugs and natural substances. The combined antifungal activity of VJ and Cz were evaluated by checkerboard dilution technique which revealed a synergistic effect between VJ and Cz against both *A. niger* and *Candida albicans*. VJ/Cz loaded chitosan nanoparticles had the highest antifungal activity with inhibition zone diameter of 72 and 74 mm against *A. niger* and *Candida albicans* respectively. The antifungal mechanism of action of the prepared nano-formula was assessed by electron microscopic study which revealed the nanoparticles precipitated and adsorbed on the fungal cell surface leading to membrane disruption and releasing of the cellular contents. The antifungal activity against fungal mat was due to the diffusion of charged nanoparticles onto the cell wall of the fungal species which eventually causes cell death (Ing et al., 2012). Chitosan nanoparticles has a metal chelating and DNA binding activities that inhibit mRNA synthesis which can attribute in the observed antimicrobial activity (Divya & Jisha, 2018). **Klis et al. (2007)** reported higher resistance activity of *A. niger* strains after chitosan nanoparticles treatment which can be expalined by the fact that *A. niger* cell wall contains 10% of chitin (the non-deacetylated form of chitosan).

In the present study, the antioxidant activity of **NCs/VJ/Cz** was 97.5% with IC_{50} reached 2.7 mg/ml. De la Cerda-Carrasco et al. (2015) tested the antioxidant activity of white *Vitis vinifera* juice extracts which presented higher antioxidant capacities and higher contents of total phenols and total proanthocyanidins compared with red *Vtis vinifera* juice extracts. Huang & Li (2014) tested the DPPH and ROS radical scavenging activity of Chitosan/fucoidan nanoparticles which showed potent antioxidant effect. Yen et al. (2008) explained that the observed antioxidant activity of chitosan was due to the iron chelating ability and hydroxyl radical scavenging activity.

The formulated NCs/VJ/Cz had a denser color in the core, which might be due to the higher phosphorous content of TPP in the cross-linked core of the nanoparticles (Abdelkader et al., 2017). FTIR spectral details of NCs/VJ/Cz (Fig. 4**a)** showed absorption band obtained at 3433.9 cm^{-1} attributed to the physical interactions with TPP when converting chitosan to a Nano particulate form (Abdelkader et al., 2017**).** Fig. 4**b** showed the X-Ray diffraction patterns of NCs loaded with VJ and Cz which showed two peaks at 2 **Θ** = 27° indicating a shift from the pure chitosan peaks around 20° revealing the increased amorphous nature of chitosan after crosslinking with sodium tripolyphosphate (Abdelkader et al., 2017). Sharma and Sharma (2013) reported that terbinafne (an antifungal agent) was effectively encapsulated in chitosan nanoparticles (77.8%).

Ex vivo and in vivo evaluation of skin retention, permeation and wound repair potentiality were examined. NCs/VJ/Cz formula was able to gradually release the drug by time. The initial burst release might be attributed to the diffusion of Cz molecules and VJ that were localized at or close to the surface of the nanoparticles. The sustained release then occurred due to the diffusion of the drug through the cross-linked Cs matrix (Ing et al., 2012). The drug flux through a membrane (dialysis bag) increases as the thermodynamic activity of the drug increases (Hemmati, 2015; Abdelkader et al., 2017). The thermodynamic activity of a drug can be increased by decreasing the drug solubility in the carrier or by increasing the drug concentration (Higuchi, 1960). Nano-formulations of drugs can enhance the drug penetration into the skin through topical application (Madheswaran et al., 2013). Ex vivo permeation studies of Egyptian Thompson Seedless *Vitis vinifera* (VJ) and Clotrimazole (Cz) from the loaded Chitosan nanoparticles (NCs/VJ/Cz) ointment revealed the enhanced drug permeation. Its incorporation into ointment reached almost a 1.5-fold permeation increase. This can be explained on the basis of the physicochemical characteristics of the prepared Nano-formula (Madheswaran et al., 2013). Both Nano-chitosan and gelatin were known for their skin penetration effect (Lou et al., 2013). In addition, the particle size of NCs/VJ/Cz could influence the ex vivo permeation of VJ and Cz (Madheswaran et al., 2013). Whereas, the smaller particle size (less than100 nm) means large

surface area which allow the drug to deeply penetrate the skin (Stoye et al., 1998). Similarly, Modi et al. (2013) prepared a ketoconazole loaded chitosan nanoparticle which showed potent sustained release over time due to highly absorption in the gastric mucosa.

The drug deposition was enhanced significantly due to high similarity between gelatin (gelation material of the prepared ointment) and the collagen present in the skin which allows the drug delivery and diffusion through the skin (Gosenca et al., 2013). Aggarwal & Goindi (2013) suggested that the rapid penetration of the drug has a significant effect in choosing the suitable skin targeting formulation. Hence, the in vivo skin deposition study through different time intervals was done. Data represented in Table 8 revealed that the VJ and Cz exhibited rapid penetration into the skin.

It is of considerable interest that animals from all the experimental groups did not exhibit any case of mortality. Wound contraction showed gradual reduction of wound area in 6 days and complete healing after 7 days (Fig. 7). Hemmati (2015) tested topical *Vitis vinifera* seed extract in a eucerin base (2% w/w) and announced that it had significant wound healing effect in rabbits and this effect was greater than that of phenytoin topical application. In this study, the hemolysis activity of the promising formula (NCs/VJ/Cz) was proved to be highly hemocompatible (0.3%). Brown et al. (2010) revealed that resveratrol (active constituent of *Vitis vinifera* seed extract) at doses of 0.5 and 1 g was completely safe and that adverse gastrointestinal effects appeared with doses of 2.5 and 5 g.

Conclusion

Chitosan nanoparticles loaded with Thompson seedless *Vitis vinifera* juice extract **(NCs/VJ/Cz)** ointment was prepared and the ex vivo and in vivo evaluation of skin retention, permeation and wound repair potentiality were examined by experimental skin fungal infected rats. Data revealed that the formula was able to gradually release the drugs in a sustained manner with tissue repairing and complete wound healing effect after 7 days. Hence, Clotrimazole combination with Thompson Seedless *Vitis vinifera* juice extract (VJ) loaded on chitosan nanoparticles can be used as novel anti-dermatophytic agent with potent wound healing capacity.

Financial & competing interests' disclosure

The authors have no relevant affiliations or financial involvement with any organization or entity with a financial interest in or financial conflict with the subject matter or materials discussed in the manuscript. This includes employment, consultancies, honoraria, stock ownership or options, expert testimony, grants or patents received or pending, or royalties.

No writing assistance was utilized in the production of this manuscript.

Declaration of Competing Interest

The authors declare that they have no known competing financial interests or personal relationships that could have appeared to influence the work reported in this paper.

Appendix A. Supplementary data

Supplementary data to this article can be found online at https://doi.org/10.1016/j.sjbs.2021.10.041.

References

Abdelkader, A., El-Mokhtar, M.A., Abdelkader, O., Hamad, M.A., Elsabahy, M., El-Gazayerly, O.N., 2017. Ultrahigh antibacterial efficacy of meropenemloaded chitosan nanoparticles in a septic animal model. Carbohyd Poly. 174, 1041–1050.

Aggarwal N, Shishu, 2006. Preparation of hydrogels of griseofulvin for dermal application. International journal of pharmaceutics 326 (1–2), 20–24. https://doi.org/10.1016/j.ijpharm.2006.07.001.

Aggarwal, N., Goindi, S., 2013. (2013) Dermatopharmacokinetic and pharmacodynamic evaluation of ethosomes of griseofulvin designed for dermal delivery. J Nanoparticle Res. 15 (10), 1983.

Altuntas, A., Yilmaz, H.R., Altuntas, A., et al., 2014. (2014) Caffeic Acid Phenethyl Ester Protects against Amphotericin B Induced Nephrotoxicity in Rats Model. Biomed Res Int. 2014, 1–8.

Arizmendi, N., Puttagunta, L., Chung, K.L., Davidson, C., Rey-Parra, J., Chao, D.V., Thebaud, B., Lacy, P., Vliagoftis, H., 2014. Rac2 is involved in bleomycin-induced lung inflammation leading to pulmonary fibrosis. Resp Res. 15, 71–83.

Basak, P., Das, P., Biswas, S., Biswas, N. C., & Mahapatra, G. K. D. (2018). Green synthesis and characterization of ointmentatin-PVA silver nanocomposite films for improved antimicrobial activity. In IOP Conference Series: Materials Science and Engineering (Vol. 410, No. 1, p. 012019). IOP Publishing.

Bonazzi, D., Cavrini, V., Gatti, R., Boselli, E., Caboni, M., 1998. Determination of imidazole antimycotics in creams by supercritical fluid extraction and derivative UV spectroscopy. Journal of pharmaceutical and biomedical analysis 18 (1-2), 235–240.

Brown, V.A., Patel, K.R., Viskaduraki, M., Crowell, J.A., Perloff, M., Booth, T.D., Vasilinin, G., Sen, A., Schinas, A.M., Piccirilli, G., Brown, K., Steward, W.P., Gescher, A.J., Brenner, D.E., 2010. Repeat dose study of the cancer chemopreventive agent resveratrol in healthy volunteers: safety, pharmacokinetics, and effect on the insulin-like growth factor axis. Cancer research 70 (22), 9003–9011.

Butani, D., Yewale, C., Misra, A., 2014. (2014) Amphotericin B topical microemulsion: formulation, characterization and evaluation. Colloids Surf B Biointerfaces. 116, 351–358.

Cavaleiro, C., Salgueiro, L., Gonçalves, M.J., Hrimpeng, K., Pinto, J., Pinto, E., 2015. Antifungal activity of the essential oil of *Anointmentica major* against *Candida, Cryptococcus, Aspergillus* and dermatophyte species. Journal of natural medicines 69 (2), 241–248.

CLSI. (2017). Performance standards for antimicrobial susbetibility testing. CLSI document M100-S26. Wayne, PA: Clinical and laboratory standards inistitute.

de la Cerda-Carrasco, A., López-Solís, R., Nuñez-Kalasic, H., Peña-Neira, Á., Obreque-Slier, E., 2015. Phenolic composition and antioxidant capacity of juice extracts from four grape varieties (*Vitis vinifera* L.). Journal of the Science of Food and Agriculture 95 (7), 1521–1527.

Divya, K., Jisha, M.S., 2018. Chitosan nanoparticles preparation and applications. Environmental chemistry letters 16 (1), 101–112.

Elnaggar, Y.SR., Elwakil, B.H., Elshewemi, S.S., El-Naggar, M.Y., Bekhit, A.A., Olama, Z. A., 2020. Novel Siwa propolis and colistin-integrated chitosan nanoparticles: elaboration; in vitro and in vivo appraisal. Nanomedicine 15 (13), 1269–1284.

El-Refaie, W.M., Elnaggar, Y.S., El-Massik, M.A., Abdallah, O.Y., 2015. Novel curcumin loaded ointment-core hyaluosomes with promising burn-wound healing potential: development, in-vitro appraisal and in-vivo studies. Int J Pharm. 486, 88–98.

Elsheikh, M.A., Elnaggar, Y.S., Gohar, E.Y., Abdallah, O.Y., 2012. Nanoemulsion liquid preconcentrates for raloxifene hydrochloride: optimization and in vivo appraisal. Inter J nanomed. 7, 37–87.

Falah-Tafti, A., 2010. A comparison of the efficacy of nystatin and fluconazole incorporated into tissue conditioner on the in vitro attachment and colonization of *Candida albicans*. Dent Res J 2010 (7), 18–22.

Foucquier, J., Guedj, M., 2015. Analysis of drug combinations: current methodological landscape. Pharmacol Res Perspect. 3, 1–10.

Fraternale, D., Ricci, D., Verardo, G., Gorassini, A., Stocchi, V., & Sestili, P. (2015). Activity of *Vitis vinifera* tendrils extract against phytopathogenic fungi. Natural product communications, 10(6), 1934578X1501000661.

Fuentefria, A.M., Pippi, B., Dalla Lana, D.F., Donato, K.K., de Andrade, S.F., 2018. Antifungals 616 discovery: an insight into new strategies to combat antifungal resistance. Lett Appl 617 Microbiol 66, 2–13.

Ge, S., Lin, Y., Lu, H., Li, Q.i., He, J., Chen, B., Wu, C., Xu, Y., 2014. (2014) Percutaneous delivery of econazole using microemulsion as vehicle: formulation, evaluation and vesicle-skin interaction. Int J Pharm. 465 (1-2), 120–131.

Ghadi, A., Mahjoub, S., Tabandeh, F., Talebnia, F., 2014. Synthesis and optimization of chitosan nanoparticles: potential applications in nanomedicine and biomedical engineering. Casp J Int Med 5 (3), 156.

Gosenca, M., Bešter-Rogač, M., Gašperlin, M., 2013. (2013) Lecithin based lamellar liquid crystals as a physiologically acceptable dermal delivery system for ascorbyl palmitate. Eur J Pharm Sci. 50 (1), 114–122.

Gupta, M., Vyas, S.P., 2012. (2012) Development, characterization and in vivo assessment of effective lipidic nanoparticles for dermal delivery of fluconazole against cutaneous candidiasis. Chem Phys Lipids. 165 (4), 454–461.

Hemmati, A.A., 2015. The topical effect of grape seed extract 2% cream on surgery wound healing. Global journal of health science 7 (3), 52.

Higuchi, T., 1960. (1960) Physical chemical analysis of percutaneous absorption process from creams and ointments. J Soc Cosmet Chem. 11 (2), 85–97.

Houillé, B., Papon, N., Boudesocque, L., et al., 2014. Antifungal activity of resveratrol derivatives against *Candida* species. J Nat Prod 77, 1658–1662.
Huang, Y.C., Li, R.Y., 2014. Preparation and characterization of antioxidant nanoparticles composed of chitosan and fucoidan for antibiotics delivery. Mar Drugs 12 (8), 4379–4398.
IACUC Faculty and Staff. (2016) Guideline on anesthesia and analgesia in laboRatsory animals. University of South Florida; [Accessed September 1, 2016]. pp. 1–20. Available from:
Ing, L., Zin, N., Sarwar, A., Katas, H., 2012. Antifungal activity of chitosan nanoparticles and correlation with their physical properties. Int J Biomater 2012, 1–9.
Jridi, M., Sellimi, S., Lassoued, K.B., Beltaief, S., Souissi, N., Mora, L., Nasri, R., 2017. Wound healing activity of cuttlefish ointmentatin ointments and films enriched by henna (*Lawsonia inermis*) extract. Colloids and Surfaces A: Physicochemical and Engineering Aspects 512, 71–79.
Katalinic, V., Mozina, S.S., Generalic, I., Skroza, D., Ljubenkov, I., Klancnik, A., 2013. Phenolic profile, antioxidant capacity, and antimicrobial activity of leaf extracts from six Vitis vinifera L. varieties. International journal of food properties 16 (1), 45–60.
Koukaras, E.N., Papadimitriou, S.A., Bikiaris, D.N., Froudakis, G.E., 2012. Insight on the Formation of Chitosan Nanoparticles through Ionotropic gelation with Tripolyphosphate. Molec Pharmac. 9, 2856–2862.
Kumar, J., Muralidharan, S., Parasuraman, S., 2014. (2014) Evaluation of antifungal activity of sustained release microsponge enriched fluconazole ointment for penile candidiasis in male rats. Int J PharmTech Res. 6 (6), 1888–1897.
Kuruc, M., Čonková, E., 2017. Synergistic effect of azole antimycotics (clotrimazole and fluconazole) and natural substances. Ceska a Slovenska farmacie: casopis Ceske farmaceuticke spolecnosti a Slovenske farmaceuticke spolecnosti 66 (4), 164–167.
Landriscina, A., Rosen, J., Friedman, A.J., 2015. Biodegradable chitosan nanoparticles in drug delivery for infectious disease. Nanomedicine 10 (10), 1609–1619.
Leonida, M.D., Belbekhouche, S., Benzecry, A., Peddineni, M., Suria, A., Carbonnier, B., 2018. Antibacterial hop extracts encapsulated in nanochitosan matrices. International journal of biological macromolecules 120, 1335–1343.
Lou, H., Qiu, N., Crill, C., Helms, R., Almoazen, H., 2013. (2013) Development of w/o microemulsion for transdermal delivery of iodide ions. AAPS PharmSciTech. 14 (1), 168–176.
Madheswaran, T., Baskaran, R., Yong, C.S., Yoo, B.K., 2013. (2013) Enhanced topical delivery of finasteride using glyceryl monooleate-based liquid crystalline nanoparticles stabilized by cremophor surfactants. AAPS PharmSciTech. 15 (1), 44–51.
Modi, J., Joshi, G., Sawant, K., 2013. Chitosan based mucoadhesive nanoparticles of ketoconazole for bioavailability enhancement: formulation, optimization, in vitro and ex vivo evaluation. Drug. Dev. Ind. Pharm. 39 (4), 540–547.
Mousafa A.F., (2006) Zygomycetes of Egypt, in Fungi of Egypt, Report, AUMC Descriptions, No. 1, Assiut, Seaward, 2006.)
Nassiri-Asl, M., Hosseinzadeh, H., 2009. Review of the pharmacological effects of *Vitis vinifera* (Grape) and its bioactive compounds. Phytother Res 2009 (23), 1197–1204.
Nina, N., Quispe, C., Jiménez-Aspee, F., Theoduloz, C., Feresín, G.E., Lima, B., Leiva, E., Schmeda-Hirschmann, G., 2015. Antibacterial activity, antioxidant effect and chemical composition of propolis from the Región del Maule, Central Chile. Molecules. 20, 18144–18167.
Nirmala, J.G., Narendhirakannan, R.T., 2011. In vitro antioxidant and antimicrobial activities of grapes (*Vitis vinifera* L) seed and skin extracts–Muscat variety. Int J Pharm Pharm Sci 3 (4), 242–249.
Oliveira, D.A., Salvador, A.A., Smânia Jr, A., Smânia, E.F., Maraschin, M., Ferreira, S.R., 2013. Antimicrobial activity and composition profile of grape (*Vitis vinifera*) juice extract s obtained by supercritical fluids. Journal of Biotechnology 164 (3), 423–432.
Ong, T.H., Chitra, E., Ramamurthy, S., Siddalingam, R.P., Yuen, K.H., Ambu, S.P., Davaman, F., 2017. Chitosan-propolis nanoparticle formulation demonstrates anti-bacterial activity against *Enterococcus faecalis* biofilms. PLoS one. 12, e0174888.
Qushawy, M., Nasr, A., Abd-Alhaseeb, M., Swidan, S., 2018. Design, optimization and characterization of a transfersomal ointment using miconazole nitrate for the treatment of *Candida* skin infections. Pharmaceutics 10 (1), 26.
Reina, G., Gismondi, A., Carcione, R., Nanni, V., Peruzzi, C., Angjellari, M., Tamburri, E., 2019. Oxidized and amino-functionalized nanodiamonds as shuttle for delivery of plant secondary metabolites: Interplay between chemical affinity and bioactivity. Applied Surface Science 470, 744–754.
Ribes, S., Fuentes, A., Talens, P., Barat, J.M., Ferrari, G., Donsì, F., 2017. Influence of emulsifier type on the antifungal activity of cinnamon leaf, lemon and bergamot oil nanoemulsions against *Aspergillus niger*. Food Control 73, 784–795.
Sahoo, S., Pani, N.R., Sahoo, S.K., 2014. (2014) Microemulsion based topical hydroointment of sertaconazole: formulation, characterization and evaluation. Colloids Surf B Biointerfaces. 120, 193–199.
Sharma, S., Sharma, S., 2013. Synthesis, characterization and determination of encapsulation efciency of chitosan nanoparticles for terbinafne. Indo Am J Pharm Res 3 (12), 1564–1567.
Simonetti, G., D'Auria, F.D., Mulinacci, N., Milella, R.A., Antonacci, D., Innocenti, M., Pasqua, G., 2019. Phenolic content and in vitro antifungal activity of unripe grape extracts from agro-industrial wastes. Natural product research 33 (6), 803–807.
Song, C.K., Balakrishnan, P., Shim, C.K., Chung, S.J., Chong, S., Kim, D.D., 2012. (2012) A novel vesicular carrier, transethosome, for enhanced skin delivery of voriconazole: characterization and in vitro/in vivo evaluation. Colloids Surf B Biointerfaces. 92, 299–304.
Song, S.H., Lee, K.M., Kang, J.B., Lee, S.G., Kang, M.J., Choi, Y.W., 2014. (2014) Improved skin delivery of voriconazole with a nanostructured lipid carrier-based hydroointment formulation. Chem Pharm Bull. 62 (8), 793–798.
Stoye, I., Schroder, K., Muller-Goymann, C.C., 1998. (1998) Transformation of a liposomal dispersion containing ibuprofen lysinate and phospholipids into mixed micelles – Physico-chemical characterization and influence on drug permeation through excised human stratum corneum. Eur J Pharm Biopharm. 46 (2), 191–200.
Tramontina, P. F. (2002). U.S. Patent Application No. 29/129,484.
Verma, S., Bhardwaj, A., Vij, M., Bajpai, P., Goutam, N., Kumar, L., 2014. (2014) Oleic acid vesicles: a new approach for topical delivery of antifungal agent. Artif Cells Nanomed Biotechnol. 42 (2), 95–101.
Vinodhini, P.A., Sangeetha, K., Thandapani, G., Sudha, P.N., Jayachandran, V., Sukumaran, A., 2017. FTIR, XRD and DSC studies of nanochitosan, cellulose acetate and polyethylene glycol blend ultrafiltration membranes. Inter J biolog macrom. 104, 1721–1729.
Xiao, H., Li, A., Li, M., Sun, Y., Tu, K., Wang, S., Pan, L., 2018. Quality assessment and discrimination of intact white and red grapes from *Vitis vinifera* L. at five ripening stages by visible and near-infrared spectroscopy. Scientia horticulturae 233, 99–107.
Xie, P.J., Huang, L.X., Zhang, C.H., Zhang, Y.L., 2015. Phenolic compositions, and antioxidant performance of olive leaf and fruit (*Olea europaea* L.) extracts and their structure–activity relationships. J. Funct. Foods. 32, 460–471.
Yen, M.T., Yang, J.H., Mau, J.L., 2008. Antioxidant properties of chitosan from crab shells. Carbohydr. Polym. 74 (4), 840–844.